Quantitative Beam Emission Spectroscopy on TEXTOR-94.

T. Soetens[1,3], R. Jaspers[2], M. Von Hellermann[2], G. Van Oost[1] and E. Desoppere[1].

[1]*Department of Applied Physics, Ghent University, Rozier 44, B-9000 Gent, Belgium.*
[2]*FOM-Institute for Plasma Physics "Rijnhuizen", Nieuwegein, The Netherlands*[*].
[3]*Plasma Physics Laboratory, Royal Military Academy, Brussels, Belgium*[*].

1. Introduction.

Neutral beams are widely used on tokamaks for plasma heating and charge exchange (CX) spectroscopy. To perform accurate CX measurements or to control the heating power, it is essential to know the species mix and beam density. Until now, the most accurate way to achieve these quantities was based on testbed measurements of the initial beam composition [1]. The local beam density during plasma operation is deduced from an attenuation code making use of the atomic-beam-stopping cross-sections (ADAS) and radial profiles for electrons and impurity ions. However, some caution is asked for, since the actual beam composition and its dependence on the acceleration voltage may have changed in the course of operation. On the other hand, the beam attenuation code generates cumulative errors, rising exponentially as we penetrate deeper into the plasma and relies on the accuracy of atomic data, electron density and concentration of impurity ions.

Beam emission spectroscopy (BES) [2,3] may provide an attractive alternative for this standard procedure promising data on local species mix and absolute beam density. Although the application of BES has been demonstrated in the past mostly as proof of principle method, the estimated errors of absolute beam densities were comparable if not higher than the values based on numerical codes. Recent progress in atomic data and a review, in particular, of beam stopping and beam emission excitation rates has given greater confidence in the validity of BES deduced values [4].

The purpose of this paper is to demonstrate that BES provides a convincing alternative with significantly lower error bars in the case of high electron line densities. The latter point is of great interest for future large fusion devices where beam attenuation errors represent the main bottle-neck for the application of active CX spectroscopy [5] and hence access to local impurity ion data (helium ash). In addition we will show that BES measurements can be used as a basis to determine power deposition profiles of the neutral beam fractions.

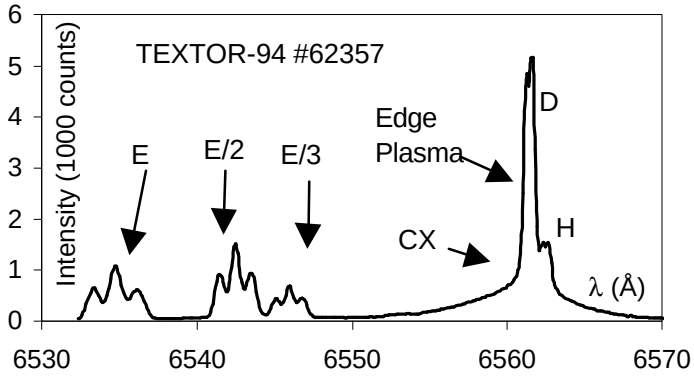

Figure 1: H_α spectrum emitted by a tokamak plasma. We can clearly separate the passive part, consisting of the Charge Exchange pedestal and the Plasma Edge emission, from the active part, emitted by the neutral beam atoms. Both the Zeeman splitting of the edge spectrum and the Motional Stark Effect of the beam spectrum are visible.

[*] Partner in the Trilateral Euregio Cluster

2. Power Fractions.

Before tackling BES itself, we will introduce the H_α spectrum, as seen on TEXTOR-94 (see figure 1, previous page). The feature we will exploit in this paper is the separation of the different structures: the passive part and the three components of the beam spectrum [2,3].
In the following paragraphs, quantities, which rely on the beam component, will be labelled with a superscript *i*, representing the beam component E/*i*. The spectrally integrated radiance of the beam components I^i is defined as:

$$I^i = \int \frac{n_e n_b^i q_{eff}^i}{4\pi} dl \tag{1}$$

n_b^i is the beam density of the E/I component. Usually, the length of integration is small, compared to the characteristic measures of the tokamak. In TEXTOR-94, this is not the case (the beam has a FWHM of 20~25 cm), but still the electron density n_e and the effective emission coefficient q_{eff}^i can be assumed constant, since the line of sight is tangential to the flux surface.
The beam line density $\int n_b^i dl$ forms the basis of further calculations. To calculate the beam power P^i we consider the kinetic energy of each beam atom. This way we find:

$$P^i = \frac{m\left(v^i\right)^2}{2} v^i \int n_b^i dS \cong A \frac{\int n_b^i dl}{i^{3/2}} \tag{2}$$

The integral $\int n_b^i dS$ describes the surface, which the neutral beam describes on the observed flux tube. The constant factor *A* in equation 2 is determined from the injected beam power.
Figure 2 represents a survey of shots with different beam acceleration voltages. In order to compare the results with testbed measurements performed by R. Uhlemann [1] (lines), we calculated relative power fractions of the beam components (markers with error bars). The beam properties are not constant in time, however we find a good agreement between the testbed results of 1994 and the BES measurements of the power fractions in 2000.

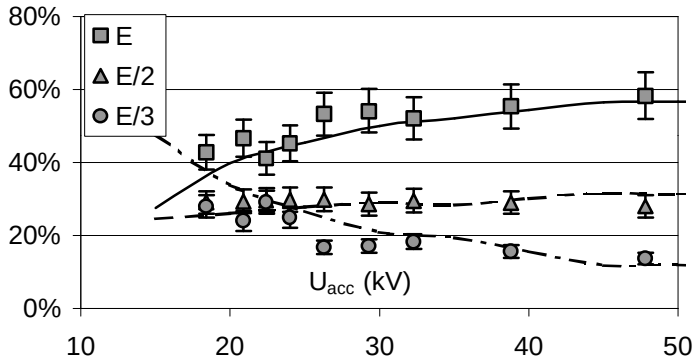

Figure 2: Injected power fractions. Comparison of the BES measurements of the outermost channel (error bars) and the testbed results (lines). We can see a good agreement.

3. Beam attenuation.

The beam attenuation ζ, calculated by the beam attenuation code, is given by:

$$\zeta = \frac{n_b}{n_{b0}} = e^{-\int n_e \sum_z \sigma_{sz} c_z dl_b} \tag{3}$$

with σ_{sz} the effective beam attenuation coefficient, c_z the impurity concentration and n_{b0} the injected beam density. The integral in equation 3 is performed over the path of the neutral beam. The beam attenuation was calculated from the BES results by dividing the local beam

density by the outermost beam density. To reduce calibration effects we re-scaled the BES results using the Bremsstrahlung.

Figure 3 shows an acceleration voltage scan of the beam attenuation. We selected the full energy (E) component of 2 lines of sight (centre and general). The lines with error bars represent the beam attenuation ζ, calculated by the beam attenuation code. The grey square markers with error bars are the values, measured by BES.

We notice a good agreement for some channels, while a discrepancy is present in the others. This tendency is also seen in other channels as well as in the E/2 and E/3 components.

The discrepancy can be addressed to different varying plasma parameters: the electron density varies from shot to shot; the effective ionic charge is not constant over the plasma profile. However, these uncertainties do not influence the BES data. Indeed we see that the error bars for BES are considerably smaller than those for the beam attenuation code in the centre of the plasma. Therefore BES is more suitable for these channels.

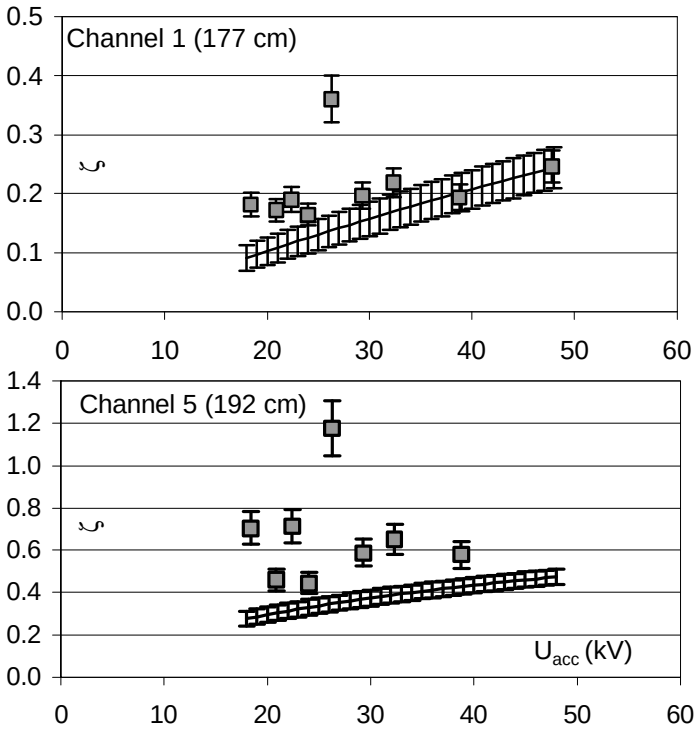

Figure 3: Beam attenuation of the full energy component in three locations. The attenuation code results are represented by the line with error bars, the BES measurements by the squares with error bars.

Figure 4 shows the relative abundance of the power fractions of the beam components. The markers with error bars show the BES measurements. The lines present values predicted by the beam attenuation code. If we compare different BES channels, we notice that the data points are scattered around the predicted values. The agreement between the BES data points and the predicted abundance proves a relative consistency and thus a relative validity of BES and of the ADAS database of atomic data for beam attenuation and emission.

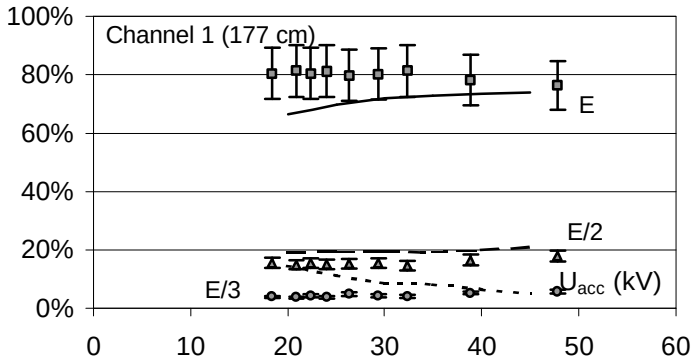

Figure 4: Relative abundance for the power fractions for a central channel. The figure shows testbed and beam attenuation code predictions (lines), BES measurements (black markers) and fit results (white markers with error bars). We notice a fair agreement between the predictions and the fit results.

4. Power deposition profiles.

The main purpose of fitting the local beam power (addressed in the previous paragraph), is the calculation of power deposition profiles:

$$S\frac{\partial P^i}{\partial V}=\frac{\partial R}{\partial r}\frac{\partial P^i}{\partial R}=\left(1-\frac{2r\delta_0}{a^2}\right)\frac{\partial P^i}{\partial R} \qquad (4)$$

S, δ_0 and a are the surface of the flux tube, the Shafranov shift of the plasma centre and the small radius of the plasma. The transformation from absolute co-ordinates to flux co-ordinates involves the Shafranov shift. The accuracy of the pressure measurements on TEXTOR-94 allows a quadratic model.

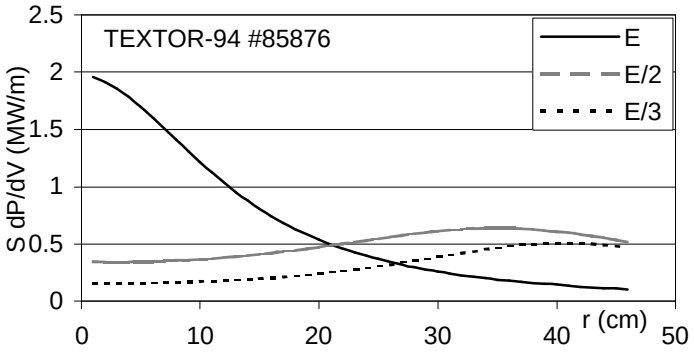

Figure 5: Power deposition profiles measured with BES. The components E, E/2 and E/3 are presented. We have taken the Shafranov shift into account.

Figure 5 shows power deposition profiles for a TEXTOR-94 discharge with a central density of 3.2 10^{19} m^{-3} and a neutral heating beam with power 0.9 MW and acceleration voltage 38.8 kV, measured with BES, after manipulation with equation 4. The figure reveals that the power deposition of the E component is highest in the centre of the plasma. However, the early attenuation of the E/2 and E/3 components makes the maximum deposition of these components to be off-axis.

5. Conclusions.

By means of beam emission spectroscopy we have measured the local beam line density of the different beam fractions. Starting from these values and taking in to account the initial beam power, we have calculated the power and the attenuation of the neutral beam fractions at different locations along the beam. Finally power deposition profiles were determined.

The BES measurements clearly confirm the testbed measurements. We also find a relative agreement between the fitted BES values and beam attenuation predictions of the power fractions for the inner channels. This is a relative confirmation of the atomic data on beam attenuation and emission.

In view of the current progress in atomic data on beam stopping and emission, and the increased experimental quality of local beam emission spectra, the application of active charge exchange spectroscopy to high density plasmas appears to be a promising option. This will not only extend the present range of impurity ion diagnostics but will also provide tools for a next-step fusion device with considerable larger dimensions and higher mean electron densities. The possibility to measure power deposition profiles of the beam components extends the application of neutral beam heating of tokamak plasmas.

References.

[1] R. Uhlemann, R.S. Hemsworth, G. Wang, H. Euringer, Rev. Sci. Instrum. **64**, 974(1993).
[2] A. Boileau et al., J. Phys. B: At. Mol. Opt. Phys., **22**, L145 (1989).
[3] W. Mandl et al., Plasma Phys. Contr. Fusion, **35**, 1373 (1993) JET-P(92)93.
[4] H. Anderson, "Collisional-Radiative Modelling of Neutral Beam Attenuation and Emission", PhD thesis, 1999.
[5] M.G. von Hellerman et al., Proc. of 1st International Workshop on ITER Diagnostics (Ed. P. Stott, G. Gorini, P. Prandoni and E. Sindoni, Plenum Press), 321-330 (1996) JET-P(95)63.